Molecular Modeling of CPT-11 Metabolism by Carboxylesterases (CEs): Use of pnb CE as a Model†

Monika Wierdl,‡ Christopher L. Morton,‡ Nathan K. Nguyen,‡ Matthew R. Redinbo,§ and Philip M. Potter*,‡

Department of Molecular Pharmacology, St. Jude Children's Research Hospital, 332 North Lauderdale, Memphis, Tennessee 38105, and Department of Chemistry, University of North Carolina at Chapel Hill, Chapel Hill, North Carolina 27599

Received September 3, 2003; Revised Manuscript Received December 9, 2003

ABSTRACT: CPT-11 is a prodrug that is converted *in vivo* to the topoisomerase I poison SN-38 by carboxylesterases (CEs). Among the CEs studied thus far, a rabbit liver CE (rCE) converts CPT-11 to SN-38 most efficiently. Despite extensive sequence homology, however, the human homologues of this protein, hCE1 and hiCE, metabolize CPT-11 with significantly lower efficiencies. To understand these differences in drug metabolism, we wanted to generate mutations at individual amino acid residues to assess the effects of these mutations on CPT-11 conversion. We identified a *Bacillus subtilis* protein (pnb CE) that could be used as a model for the mammalian CEs. We demonstrated that pnb CE, when expressed in *Escherichia coli*, metabolizes both the small esterase substrate *o*-NPA and the bulky prodrug CPT-11. Furthermore, we found that the pnb CE and rCE crystal structures show an only 2.4 Å rmsd variation over 400 residues of the α-carbon trace. Using the pnb CE model, we demonstrated that the "side-door" residues, S218 and L362, and the corresponding residues in rCE, L252 and L424, were important in CPT-11 metabolism. Furthermore, we found that at position 218 or 252 the size of the residue, and at position 362 or 424 the hydrophobicity and charge of the residue, were the predominant factors in influencing drug activation. The most significant change in CPT-11 metabolism was observed with the L424R variant rCE that converted 10-fold less CPT-11 than the wild-type protein. As a result, COS-7 cells expressing this mutant were 3-fold less sensitive to CPT-11 than COS-7 cells expressing the wild-type protein.

CPT-11[1] is a water soluble camptothecin analogue that has exhibited remarkable antitumor activity in clinical trials against a variety of human tumors (*1*−*3*) and is currently approved for the treatment of colorectal cancer. The antitumor effect is due to the *in vivo* conversion of CPT-11 to its active metabolite, SN-38, a potent topoisomerase I poison that generates stable complexes between topoisomerase I and the DNA (*4*). During cell division, these DNA−enzyme complexes collide with the advancing replication forks leading to the formation of double-strand breaks. Thus, SN-38 appears to be an S-phase specific cytotoxic agent (*2*).

The conversion of CPT-11 to SN-38 is primarily catalyzed by carboxylesterases (CEs) (*5*−*7*). CEs are members of the α/β-hydrolase superfamily, and are found in both eukaryotic and prokaryotic species (*8*, *9*). Although CEs are primarily involved in the detoxification of xenobiotics in higher eukaryotes (*10*−*12*), their role as activators of various prodrugs is important in humans (*13*, *14*).

The CEs that are involved in CPT-11 conversion in the human body have not been fully characterized; however, the human liver carboxylesterase (hCE1) and the human intestinal CE (hiCE or hCE2) have been proposed as candidate enzymes for this process (*15*, *16*). Furthermore, several other mammalian CEs have been isolated, and their CPT-11 converting abilities have been determined (*5*, *7*, *15*, *17*). These studies revealed that mammalian CEs often share extensive sequence or structural homology, but they exhibit significant differences in their ability to metabolize CPT-11. In general, rodent CEs are more efficient at drug conversion than their human homologues (*6*, *15*, *16*). For example, Danks *et al*. (*15*) demonstrated that a rabbit liver CE (rCE) is at least 100-fold more efficient in CPT-11 conversion than its human homologue, hCE1, despite the amino acid sequences being 81% identical. Interestingly, hiCE, which is only 48% identical to rCE, metabolizes CPT-11 significantly more efficiently than hCE1 (*13*, *16*).

To understand these differences in CPT-11 metabolism among the highly homologous mammalian CEs, we wanted to assess the role of specific amino acid residues in substrate recognition and CPT-11 conversion by mutational analysis. On the basis of the recently published crystal structure of the highly efficient rCE, several amino acid residues have

† This work was supported in part by NIH Grants CA-76202, CA-79763, and CA-98468, by Cancer Center Core Grant P30 CA-21765, and by the American Lebanese Syrian Associated Charities.

* To whom correspondence should be addressed: Department of Molecular Pharmacology, St. Jude Children's Research Hospital, 332 N. Lauderdale, Memphis, TN 38105. Fax: (901) 495-4293. E-mail: phil.potter@stjude.org.

‡ St. Jude Children's Research Hospital.

§ University of North Carolina at Chapel Hill.

[1] Abbreviations: CPT-11, 7-ethyl-10-[4-(1-piperidino)-1-piperidino]-carbonyloxycamptothecin (Irinotecan); SN-38, 7-ethyl-10-hydroxy-camptothecin; 4PP, 4-piperidinopiperidine; CE, carboxylesterase; hCE1, human liver carboxylesterase 1; hiCE, hCE2 human intestinal carboxylesterase; rCE, rabbit liver carboxylesterase; pnb CE, *p*-nitrobenzyl carboxylesterase; *o*-NP, *o*-nitrophenol; *o*-NPA, *o*-nitrophenyl acetate; IC_{50}, concentration of drug required to inhibit cell growth 50%.

10.1021/bi035586r CCC: $27.50
Published on Web 01/29/2004

been predicted to be involved in CPT-11 metabolism (*14*). According to the author's model, the two products of CPT-11 cleavage, SN-38 and 4-piperidinopiperidine (4PP), exit from the active site via two different routes. SN-38 is removed through the active site gorge. 4PP, however, is removed via a unique exit pore, the "side door". Since the timely removal of the small 4PP molecule from the enzyme surface was thought to be essential for CPT-11 catalysis, we chose to evaluate the possible role of four amino acid residues surrounding the side door in this process.

Since generation, expression, and purification of mutant proteins in *Escherichia coli* are much faster than in mammalian systems, we wanted to identify a bacterial model that could be used for the studies of mammalian CEs. On the basis of structural homology to rCE, we isolated the *Bacillus subtilis* protein pnb CE, and used this model to demonstrate that two side-door residues in pnb CE (S218 and L362), and the corresponding residues in rCE (L252 and L424), are important in drug recognition and catalysis. Our studies revealed important structural and functional similarities between the bacterial and mammalian CEs that provide further insights into the mechanism of CPT-11 activation by these enzymes.

MATERIALS AND METHODS

Bacterial Strains and Plasmids. *B. subtilis* (ATCC 6633) was purchased from American Type Culture Collection (ATCC). XL-1Blue supercompetent cells were obtained from Stratagene, and the *E. coli* expression host strain, Origami B(DE3)pLacI, was purchased from Novagen. The cloning vector pCRII-TOPO was obtained from Invitrogen, and the expression vector pTriEx-3 was purchased from Novagen. The expression of the *pnbA* gene in *E. coli* was accomplished by ligating the coding sequence into pTriEx-3.

Mammalian Cell Lines. COS-7 cells were obtained from ATCC, and were propagated in DMEM containing 10% FBS and 2 mM glutamine in an atmosphere of 10% CO_2 at 37 °C. Transient transfections and growth inhibition assays to determine the IC_{50} values for CPT-11 and SN-38 were performed as previously described (*7*).

pnbA Isolation and Mutagenesis. The *pnbA* gene encoding pnb CE was isolated by PCR from *B. subtilis* genomic DNA using the following primers: CCGGATCCCATGACTCATCAAATAGTAACG and CCGGATCCTTATTCTCCTTTTG. The PCR primers attached *Bam*HI restriction sites to the pnb A coding sequence for easy insertion into pTriEx-3, to create pTriEx-3/pnbA.

Random mutations in pnbA were generated by the QuickChange site-directed mutagenesis kit (Stratagene) using degenerate primers, and pTriEx-3/pnbA as a template. All primers were designed according to the manufacturer's protocol. In general, primers were 30−34 nucleotides long and at least 40% GC rich, and all mutations were designed to be in the middle of the oligonucleotides. Mutations were also created in the rabbit liver CE cDNA in the vector pCIRAB (*7*) using the same protocol, with PCR primers that created single-amino acid changes. All mutations were confirmed by DNA sequencing.

Protein Expression. *(1) Bacteria*. The wild-type and mutant pnb CE proteins were expressed in *E. coli* Origami B cells. Typically, 20 mL of LB medium containing the appropriate antibiotics was inoculated with a 1:20 dilution of an overnight bacterial culture. After the culture had grown for 3 h, target protein expression was induced with 1 mM IPTG. Cells were harvested 3−4 h following induction, and protein extracts were prepared using 10 volumes of Bug-Buster reagent (Novagen). Protein expression was confirmed by Nu PAGE SDS−PAGEs followed by SyproRuby protein gel staining (Molecular Probes), and scanning with a Storm Phosphorimager. CE expression was quantified by densitometric analysis using ImageQuant software (Molecular Dynamics). Since protein gels were loaded with samples containing equal amounts of total protein, and the expression level of the wild-type pnb CE sample on each gel was set arbitrarily to 1, we could determine the relative CE expression ratios between the different samples based on the densitometric data.

(2) Mammalian Cells. Wild-type and mutant rCE proteins were expressed in COS-7 cells by transient transfection, and cell extracts were prepared by sonication in 50 mM Hepes (pH7.4), 48 h after electroporation. Protein expression was confirmed by Western blot analysis. Cell extracts were separated on 4 to 12% precast SDS−PAGE gels (Invitrogen), and transferred to an Immobilon-P (Millipore) membrane by electroblotting. CEs were detected with an antibody directed to the C-terminal residues of hCE1 and horseradish peroxidase-conjugated anti-rabbit secondary antibodies (Amersham-Pharmacia).

Protein Purification. CEs were purified by preparative isoelectric focusing (Bio-Rad) using Bio-Lyte ampholytes 3/5. Protein extracts were prepared from 1 L of bacterial culture as described previously, and dialyzed in 10 mM Hepes (pH 7.4) prior to isoelectric focusing. After focusing had been carried out, protein fractions were tested for purity and CE activity, and the fractions containing high levels of CE activity were pooled. The ampholytes were removed by dialysis in 10 mM Hepes (pH 7.4) following the addition of 1 M NaCl to the sample. To determine the molecular weight of each protein, a sample was applied to a calibrated Sephacryl S-500 high-resolution gel filtration chromatography column (Amersham-Pharmacia).

CE Assay. CE activities were determined by a spectrophotometric assay using *o*-NPA as a substrate (*18*, *19*). Generally, protein samples were incubated with 3 mM *o*-NPA in 50 mM Hepes (pH 7.4), and the change in A_{420} was measured spectrophotometrically. Using the relative CE expression ratios that were determined by densitometric analysis of SyproRuby-stained SDS−PAGE gels or Western blots (as described above), the CE activities that were measured as micromoles of *o*-NP produced per minute per milligram of total protein were then normalized to micromoles of *o*-NP produced per milligram of CE.

CPT-11 Conversion. The ability of CEs to convert CPT-11 to SN-38 was determined by incubating samples with 50 μM CPT-11 for 1 h at 37 °C in 50 mM Hepes (pH 7.4). Reactions were terminated by addition of an equal volume of acid methanol, and the concentration of SN-38 was determined by HPLC (*19*). Reactions using rCE were performed in an identical manner except that the concentration of CPT-11 was 5 μM. Using the relative CE expression ratios (determined as described above), the measured SN-38 production was normalized from the amount of SN-38 produced per hour per milligram of total protein to the

amount of SN-38 produced per milligram of CE.

o-NPA Kinetics. K_m and V_{max} values were determined by incubating constant amounts of the protein with concentrations of *o*-NPA ranging from 3 μM to 3.5 mM for pnb CE, from 10 μM to 6 mM for S218R pnb CE, and from 50 μM to 14 mM for L362R pnb CE. The conversion of *o*-NPA to *o*-NP was followed spectrophotometrically at 420 nm for 15 s, and the reaction velocities were calculated from the linear regression of the data points. The kinetic parameters and r^2 values were determined from hyperbolic curve fits generated with Prism software (Graph Pad). K_{cat} and catalytic efficiencies were calculated as previously described (*20*, *21*).

CPT-11 Kinetics. K_m and V_{max} values were determined by incubating constant amounts of purified pnb CE with concentrations of CPT-11, ranging from 1 to 100 μM for 2 min at 37 °C in 50 mM Hepes (pH 7.4). Reactions were terminated by addition of an equal volume of acid methanol, and the amounts of SN-38 were determined by HPLC. For the mutant L362R, the purified enzyme was incubated with CPT-11 at concentrations ranging from 2 μM to 2 mM for 10 min at 37 °C, and the samples were processed as described above. All data points were performed in triplicate. The kinetic parameters and r^2 values were determined from allosteric curve fits generated with Prism software, and the catalytic efficiencies were calculated as described above. The number of substrate binding sites was determined by the linear plot of the Monod−Wyman−Changeux model proposed by Horn and Bornig (*22*).

Viscosity Measurements. Relative viscosities ($\eta_{rel} = \eta/\eta°$) of buffer solutions containing 7, 15, 23, and 30% (w/w) sucrose were determined with an Ostwald viscometer using 50 mM Hepes buffer (pH 7.4) without a viscogen as a reference. The approximate relative viscosities at 22 °C for the 7, 15, 23, and 30% (w/w) sucrose solutions were 1.29, 1.73, 2.7, and 3.94, respectively. At 37 °C, the relative viscosities were 1.15, 1.56, 2.22, and 3.21, respectively. Kinetic parameters for pnb CE and L362R pnb CE, in the presence of sucrose, were determined as described above using *o*-NPA or CPT-11 as a substrate. Quantitative evaluation of the viscosity dependence of the enzyme reactions was carried out as described previously (*23*, *24*).

Protein Structure Models. The structural coordinates of rCE and pnbA CE (PDB entries 1K4Y and 1QE3, respectively) were overlaid using DALI. Homologous residues and ribbon models were identified using Molsoft ICMPro software.

RESULTS

Identification of a Bacterial Model for Mammalian CEs. To identify amino acid residues in mammalian CEs that are involved in the activation of CPT-11, we wanted to generate mutations that specifically altered the enzyme's efficiency in metabolizing CPT-11, without greatly affecting the CE activity. Thus, following mutagenesis, we needed to evaluate each potential mutant protein for its ability to metabolize the small esterase substrate *o*-NPA, and to convert CPT-11 to SN-38. Because of the lack of a suitable selection assay for identifying such specific mutations, in addition to the difficulty of generating, expressing, and purifying mutant proteins in mammalian systems, we chose a bacterial system that could be used as a model for mammalian CEs.

Table 1: CE Activity and CPT-11 Conversion Activity of rCE and pnb CE

protein	CE activity [μmol min^{-1} (mg of CE)$^{-1}$]	CPT-11 conversion [nmol min^{-1} (mg of CE)$^{-1}$]	sequence identity to rCE (%)
rCE	35166 ± 685	20.1	−
pnb CE	19686 ± 1752	15.9	81

We searched the protein structure database (Protein Data Bank) for homology to the structural coordinates of rCE, and we identified a protein from *B. subtilis*, pnb CE, that showed an only 2.4 Å rmsd variation over 400 residues of the α-carbon trace when compared to the rabbit protein. We hypothesized that this enzyme might activate CPT-11 and could be used as a model system to rapidly analyze the effects of specific mutations in CEs.

Isolation and Expression of pnb CE. The *pnbA* gene encoding pnb CE was isolated by PCR using *B. subtilis* genomic DNA as a template. The *pnbA* clone was sequenced multiple times and was found to encode the 470 amino acid residues of pnb CE; however, there were 11 amino acid residues that were different from the published protein sequence (*25*). Repeated PCR analyses using high-fidelity polymerases (e.g., *Pfu* DNA polymerase) followed by DNA sequencing confirmed our previous results, suggesting that the observed differences in amino acid sequences represent genomic DNA sequence substitutions present among the various *B. subtilis* strains.

The *pnbA* gene was inserted into the expression vector pTriEx-3 to create pTriEx-3/pnbA. The advantage of this expression vector is that it provides high levels of protein expression both in mammalian cells and in bacteria. We expressed pTriEx-3/pnbA both in *E. coli* (Origami B) and in COS-7 cells, and found that pnb CE could metabolize both the small esterase substrate *o*-NPA and the bulky prodrug CPT-11. Comparison of the purified pnb CE and rCE revealed comparable CE activities and CPT-11 conversion efficiencies for the two proteins (Table 1). These results combined with the close structural homology between pnb CE and rCE (Figure 1A) suggested that pnb CE might be a suitable model for studying mammalian CEs.

Mutational Analysis of the Side-Door Residues in pnb CE. Recently, the three-dimensional structure of rCE was determined in the presence of 4-piperidinopiperidine (4PP) (*14*). The position of 4PP in the crystal structure, and its proximity to the active site Ser residue, suggested the existence of a unique pore, a side door that would facilitate the removal of small molecules from the active site. Furthermore, amino acid residues L252, S254, I387, and L424 surrounding the exit pore were designated side-door residues, and were suggested to be involved in CPT-11 metabolism (Figure 1B). Thus, we assessed the possible role of the side-door residues in drug activation using the pnb CE model.

Using ICMPro software, we have overlaid the rCE and pnb CE structural coordinates and identified the side-door residues in pnb CE. Residues L252, S254, I387, and L424 in rCE corresponded to amino acids S218, R219, I270, and L362 in pnb CE, respectively (Figure 1C). Our goal was to identify mutations that specifically affected the CPT-11 metabolism of pnb CE. Thus, we used degenerate primers to create random mutations at these side-door residues in pnb CE. Mutant CEs were identified by DNA sequencing,

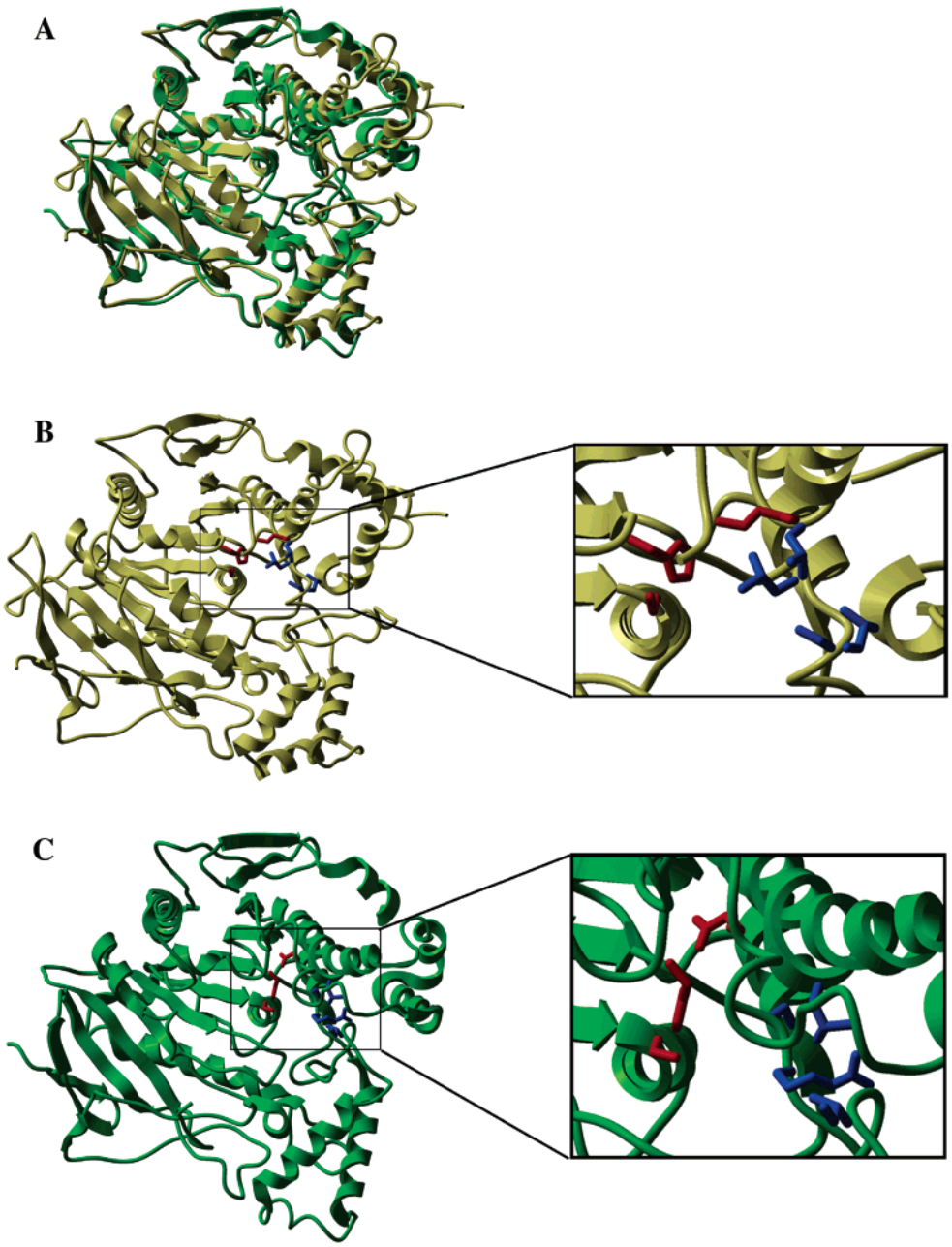

FIGURE 1: (A) Overlay of ribbon diagrams of rCE (gold) and pnb CE (green). Proteins were overlaid using ICMPro software using the X-ray coordinates of both enzymes. (B) Crystal structure of rCE. Active site residues S221, E353, and H467 are shown in red, and side-door residues L252, S254, I387, and L424 are shown in blue. (C) Crystal structure of pnb CE. Active site residues S189, E310, and H399 are shown in red. Residues corresponding to the side-door residues in rCE (S218, R219, I270, and L362) are shown in blue.

and following expression in *E. coli*, their CE activity and ability to activate CPT-11 were determined.

Analysis of the mutant pnb CE proteins demonstrated that the four residues corresponding to the side-door residues of rCE were not equally sensitive to mutagenesis. Table 2 indicates that substitution of the hydrophobic aliphatic L362 residue to a positively charged hydrophilic Arg or Lys amino acid inhibited CPT-11 metabolism 10- or 5-fold, respectively, with only a moderate decrease in CE activity. Although modest effects on *o*-NPA catalysis were observed with other amino acid substitutions (e.g., Trp and Pro), their influence on CPT-11 activation was minimal. Overall, only the L362R and L362K mutants demonstrated significant differences in drug activation (Table 2).

At amino acid residue S218, several substitutions inhibited the catalysis of CPT-11 by 3−5-fold, coupled with a 2−3-fold decrease in CE activity (Table 3). These amino acid changes included both hydrophilic (Arg) and hydrophobic (Phe, Tyr, Trp, and Leu), and aliphatic (Leu) and aromatic (Phe, Tyr, and Trp), residues. The common characteristic among these residues, as shown in Table 3, is that their volume is greater than 166 Å^3. Interestingly, a decrease in residue volume from 89 to 60.1 Å^3 with the S218G substitution did not improve the enzyme's ability to metabolize CPT-11. On the contrary, the S218G substitution led to 5- and 3-fold inhibition of *o*-NPA and CPT-11 conversion, respectively (Table 3).

Mutation of amino acids at positions 219 and 270 in *B. subtilis* pnb CE, which correspond to residues S254 and I387 in rCE, respectively, essentially had no effect on either CE activity or CPT-11 catalysis (data not shown). The only exception was an R219P substitution that decreased the CE

Table 2: Effects of Mutations at L362 on CE Activity and CPT-11 Conversion

amino acid	CE activity (μmol min^{-1} mg^{-1} ± SD)	CPT-11 conversion (nmol h^{-1} mg^{-1} ± SD)	fold decrease in CE activity from the wild-type value	fold decrease in CPT-11 conversion from the wild-type value
Leu (wild type)	33315 ± 4961	36.0 ± 9.7		
Val	23393 ± 1771	29.9	1.4	1.2
Gly	33445 ± 2822	46.2	1.0	0.8
Ala	33231 ± 1699	32.4	1.0	1.1
Ile	24095 ± 1850	36.6	1.4	1.0
Pro	17947 ± 1794	20.3	1.9	1.8
Phe	34814 ± 2116	57.6	1.0	0.6
Tyr	25341 ± 678	54.0	1.3	0.7
Trp	43147 ± 2249	54.0	0.8	0.7
Cys	36448 ± 3283	34.6	0.9	1.0
Ser	25723 ± 1312	32.1	1.3	1.1
Thr	24304 ± 1085	33.3	1.4	1.1
Lys	**18454 ± 1524**	**6.8**	**1.8**	**5.3**
Arg	**13348 ± 1130**	**3.4**	**2.5**	**10.6**
His	21868 ± 3242	70.4	1.5	0.5
Asn	30740 ± 877	26.3	1.1	1.4
Gln	19556 ± 1355	28.2	1.7	1.3
Glu	25630 ± 262	48.0	1.3	0.8
Asp	26838 ± 1900	26.2	1.2	1.4

Table 3: Effects of Mutations at S218 on CE Activity and CPT-11 Conversion

amino acid	CE activity (μmol min^{-1} mg^{-1} ± SD)	CPT-11 conversion (nmol h^{-1} mg^{-1} ± SD)	fold decrease in CE activity from the wild-type value	fold decrease in CPT-11 conversion from the wild-type value	residue volume (Å^3)
Ser (wild type)	35305 ± 4871	33.0 ± 4.8			89.0
Gly	6924 ± 452	10.4	5.1	3.2	60.1
Ala	17376 ± 784	21.8	2.0	1.5	88.6
Leu	**16483 ± 807**	**10.1**	**2.1**	**3.3**	**166.7**
Ile	**22999 ± 869**	**10.4**	**1.5**	**3.2**	**166.7**
Pro	25299 ± 1225	16.2	1.4	2.0	112.7
Phe	**17116 ± 521**	**7.0**	**2.1**	**4.7**	**189.9**
Tyr	**10787 ± 566**	**7.0**	**3.3**	**4.7**	**193.6**
Trp	**13638 ± 1364**	**9.3**	**2.6**	**3.5**	**227.8**
Cys	19901 ± 1711	15.9	1.8	2.1	108.5
Thr	27374 ± 175	21.2	1.3	1.6	116.1
Arg	**21199 ± 138**	**7.4**	**1.7**	**4.5**	**173.4**
Lys	**31563 ± 781**	**9.0**	**1.1**	**3.4**	**168.6**
Gln	19979 ± 287	19.6	1.8	1.7	143.8
Asn	25454 ± 1237	17.1	1.4	1.9	114.1
Glu	27219 ± 2244	17.5	1.3	1.9	138.4

Table 4: CE Activities, CPT-11 Conversion Activities, and IC_{50} Values for COS-7 Cells Expressing Wild-Type or Mutant rCEs

COS-7 cell extract	CE activity [μmol min^{-1} (mg of CE)$^{-1}$]	fold change	CPT-11 conversion [pmol min^{-1} (mg of CE)$^{-1}$]	fold change	CPT-11 IC_{50} (μM)	fold change	SN-38 IC_{50} (nM)	fold change
rCE	662.07		112.3		7.4		52	
L424R rCE	266.67	2.5	8.0	14	28.8	3.9	68	1.3
rCE	926.1		129.4		6.5		ND[a]	
L252R rCE	226.4	4.1	43.0	3.0	15.7	2.4	ND[a]	

[a] Not determined.

activity and extent of CPT-11 conversion 5.6- and 3.2-fold, respectively, suggesting that the effect of this mutation was more significant on *o*-NPA conversion than on CPT-11 metabolism.

Overall, these results suggest that S218 and L362 are both important in CPT-11 catalysis. However, at position 362, the charge and hydrophobicity of the amino acid appear to be the predominant factors that influence drug activation. At position 218, the electrostatic charge and lipophilicity of the residue appear to be less important, with the size of the amino acid being the primary determinant in regulating CE-mediated metabolism.

Mutation of the L424 and L252 Side-Door Residues in rCE. To confirm that pnb CE was a valid model system for studying mammalian CEs, we generated the L424R and L252R mutations in rCE that corresponded to the L362R and S218R mutations in pnb CE. We expressed the wild-type and mutant rCE proteins in COS-7 cells, and measured their CE activity and CPT-11 conversion activity in cell extracts. We also compared the CPT-11 sensitivity of COS-7 cells that expressed either the wild-type, L424R, or L252R rCE. As Table 4 indicates, the L424R rCE mutant protein had 2.5-fold less esterase activity and 14-fold weaker ability to convert CPT-11 than the wild-type protein. As a result,

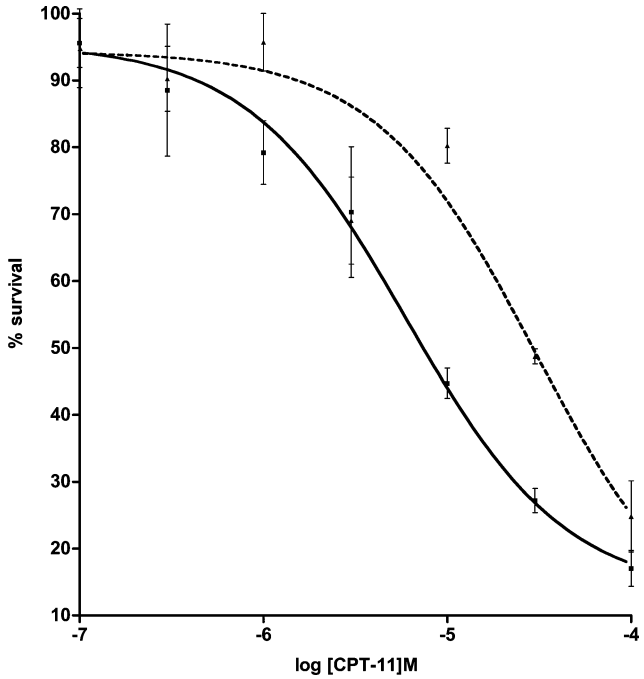

FIGURE 2: Growth inhibition curves for COS-7 cells expressing rCE (—) or L424R rCE (- - -) following treatment with CPT-11.

COS-7 cells that expressed L424R rCE were approximately 4-fold less sensitive to CPT-11 than cells that expressed rCE (Figure 2). No change in the sensitivity of the cells to SN-38 was observed (Table 4), indicating that the reduction in cytotoxicity toward CPT-11 was due to expression of the CE, and not due to an alteration in the levels of topoisomerase I and/or accumulation of the drug.

The L252R rCE mutant also demonstrated a reduced CE activity and level of CPT-11 conversion when compared to wild-type rCE (Table 4). However, the efficiency of *o*-NPA and CPT-11 hydrolysis decreased by only 4.1- and 3-fold, respectively. Consistent with these results, COS-7 cells that expressed L252R were ~2-fold less sensitive to CPT-11 than those that expressed rCE. Thus, mutant rCEs containing substitutions in residues that form the side door demonstrated phenotypes similar to the corresponding mutant pnb CE proteins. These results suggest that pnb CE is a valuable model for analyzing the mechanism of catalysis of different substrates by mammalian CEs.

Purification and Kinetic Parameters of pnb CE and L362R pnb CE. To further characterize the effect of the L362R mutation on substrate catalysis, we purified both the wild-type and mutant proteins by preparative isoelectric focusing.

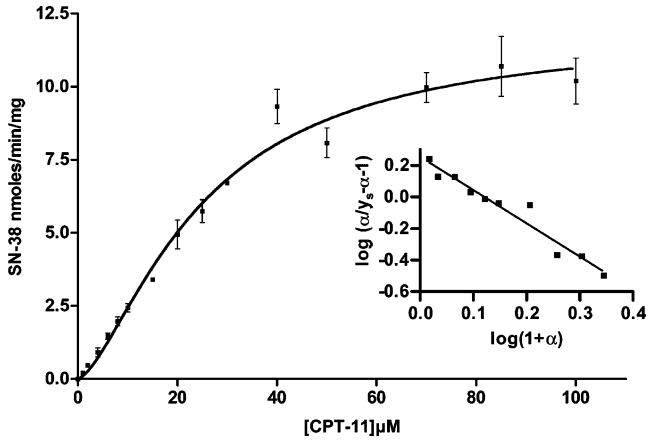

FIGURE 3: Sigmoidal velocity curve for wild-type pnb CE using CPT-11 as a substrate. The inset shows a Horn—Borning plot for pnb CE (■), where $\alpha = s/K_s$, $Y_s = v/V_{max}$, and the number of binding sites is determined from the slope of the line [slope $= -(n - 1)$].

Analysis of each protein on a calibrated Sephacryl S-500 high-resolution gel filtration chromatography column revealed that in solution, both enzymes existed as a mixture of monomers and trimers. Additionally, we found that the trimers represented the significant proportion of these mixtures.

Kinetic parameters for *o*-NPA were determined by assessing the conversion of *o*-NPA to *o*-NP. Both enzymes exhibited standard Michaelis—Menten kinetics. As shown in Table 5, a 10-fold increase in the K_m value was observed for the L362R mutant CE compared to that of the wild-type protein. The V_{max} for L362R CE was only 1.2-fold greater than that for the wild-type protein, resulting in an 8-fold decrease in the catalytic efficiency of the mutant CE as compared to the wild-type enzyme.

The kinetics of CPT-11 metabolism showed more significant differences between the wild-type and mutant proteins (Table 6). We found that neither enzyme exhibited Michaelis—Menten kinetics. The substrate velocity curves of both enzymes were sigmoidal, representing allosteric enzyme kinetics, and multiple binding sites for CPT-11 (Figure 3). The apparent Hill coefficient was 1.5 for the wild type and 1.8 for the L362R mutant enzyme, indicating positive cooperativity among the enzyme drug binding sites. The actual number of CPT-11 binding sites was determined to be three by the linear plot of the Monod—Wyman—Changeuw model described by Horn and Borning (*22*) (see Figure 3). These findings, and our previous observations that

Table 5: Kinetic Parameters of pnb CE, L362R pnb CE, and L218R pnb CE Using *o*-NPA as a Substrate

protein	K_m (μM)	V_{max} (μmol min^{-1} mg^{-1})	curve fit (r^2)	k_{cat} (s^{-1})	k_{cat}/K_m (s^{-1} mM^{-1})
pnb CE	701 ± 75.61	84.60 ± 3.11	0.98	76.22	108.71
L362R pnb CE	7138 ± 1480	103.31 ± 11.4	0.96	93.07	13.04
L218R pnb CE	1175 ± 138.0	47.72 ± 2.68	0.98	56.07	47.72

Table 6: Kinetic Parameters of pnb CE and L362R pnb CE Using CPT-11 as a Substrate

protein	H_{app}	K_m (μM)	V_{max} (nmol min^{-1} mg^{-1})	curve fit (r^2)	k_{cat} (s^{-1})	k_{cat}/K_m (s^{-1} mM^{-1})
pnb CE	1.51	24.7 ± 2.9	14.0 ± 0.75	0.96	0.0126	0.511
L362R pnb CE	1.81	267.4 ± 6.29	0.86 ± 0.02	0.99	0.0008	0.003

Table 7: Effect of Sucrose Concentration on the Kinetic Parameters of pnb CE and L362R pnb CE

		fold increase				
substrate	parameter	0% sucrose	7% sucrose	15% sucrose	23% sucrose	30% sucrose
o-NPA	K_m (pnb CE)	1	0.88 ± 0.13	0.75 ± 0.10	0.65 ± 0.09	0.45 ± 0.09
	k_{cat} (pnb CE)	1	0.77 ± 0.04	0.65 ± 0.03	0.58 ± 0.02	0.42 ± 0.02
	K_m (L362R pnb CE)	1	0.90 ± 0.03	0.63 ± 0.04	0.39 ± 0.02	0.40 ± 0.02
	k_{cat} (L362R pnb CE)	1	0.84 ± 0.01	0.59 ± 0.02	0.41 ± 0.01	0.36 ± 0.01
CPT-11	K_m (pnb CE)	1	2.15 ± 0.12	2.88 ± 0.22	ND[a]	3.54 ± 0.37
	k_{cat} (pnb CE)	1	1.36 ± 0.03	1.36 ± 0.3	ND[a]	1.27 ± 0.05
	K_m (L362R pnb CE)	1	1.24 ± 0.07	1.6 ± 0.1	ND[a]	1.97 ± 0.10
	k_{cat} (L362R pnb CE)	1	0.99 ± 0.02	0.83 ± 0.03	ND[a]	0.86 ± 0.02

[a] Not determined.

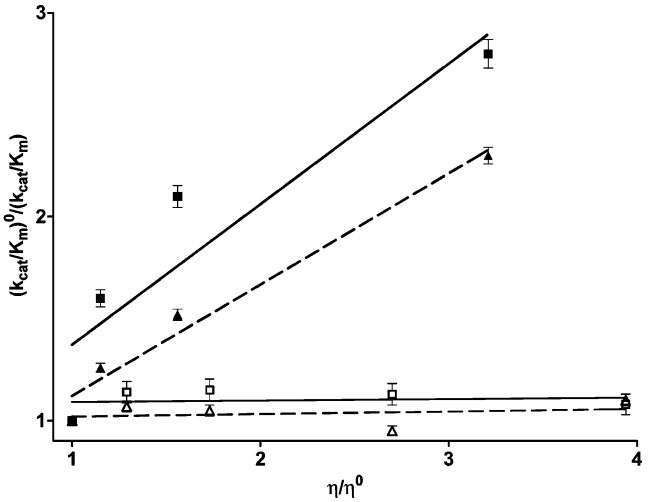

FIGURE 4: Effect of sucrose on the hydrolysis of *o*-NPA or CPT-11 by pnb CE or L362R pnb CE. White symbols represent measurements using *o*-NPA as a substrate with pnb CE (□) or L362R pnb CE (△). Black symbols represent measurements using CPT-11 as a substrate with pnb CE (■) or L362R pnb CE (▲).

pnb CE and L362R pnb CE exist in solution primarily as trimers, suggest that both proteins have a single CPT-11 binding site per monomer.

With the L362R mutant, we observed a 10-fold increase in K_m and a 16-fold decrease in V_{max} when CPT-11 was used as the substrate (Table 6). As a result, the catalytic efficiency of this CE was 170-fold lower than that of wild-type pnb CE. Thus, the L362R substitution had significantly different effects on CPT-11 catalysis and *o*-NPA hydrolysis.

Viscosity Variation Experiments. To determine whether *o*-NPA or CPT-11 catalysis was limited by diffusive processes, by either substrate association or product release, we repeated our kinetic experiments in the presence of different concentrations of sucrose. We determined the relative changes in the kinetic parameters as a function of viscogen concentration, using values measured without sucrose as a reference. As shown in Table 7, the effect of the increasing viscosity was significantly different for the two substrates. In the case of *o*-NPA, the increase in sucrose concentration resulted in a decrease in both K_m and k_{cat} values; however, their ratios essentially did not change. The independence of k_{cat}/K_m from the changes in relative viscosity (Figure 4) suggested that *o*-NPA hydrolysis by either the wild-type or mutant enzyme was not limited by diffusion. With CPT-11, however, we observed a change in the second-order rate constant as a function of viscosity, indicating that cleavage of this substrate is partially controlled by diffusion (Figure 4). Furthermore, increasing the viscosity of the reaction buffer resulted in a steady increase in the K_m value without substantial changes in k_{cat}, suggesting that substrate association rather than product diffusion was rate-limiting. Quantitative evaluation of the viscosity dependence observed with CPT-11, by the method of Nakatani and Dunford (*23*), revealed a 137-fold difference in the rate constants for substrate association between pnb CE and L362R pnb CE. These values were 0.725 and 0.0053 mM^{-1} s^{-1} for the two enzymes, respectively, and in both cases, the partition ratios were identical, with a value of 1.

DISCUSSION

We are interested in the mechanism and efficiency of CPT-11 metabolism by mammalian CEs. The results presented here indicate that a bacterial protein can be used as a model for the rapid analysis of specific mutations and their effects on drug catalysis. In addition, the comparable phenotypes of the corresponding mutations made within pnb CE and rCE demonstrate a common function for specific amino acid residues between the bacterial and mammalian CEs. Our results provide the first evidence supporting the assumption that the side door and surrounding residues might be important in CE-mediated CPT-11 catalysis. The existence of a side door that facilitates the removal of small molecules from the enzyme's surface has been predicted from the three-dimensional structure of rCE (*14*). A "back door" with similar functions was also suggested on the basis of the crystal structure of acetylcholinesterases (*26*, *27*). However, experimental evidence to support these hypotheses has not been presented thus far.

We created random mutations at the pnb CE side-door residues and found that the S218 and L362 residues are both involved in CPT-11 metabolism; however, their role is different. At S218, the size of the amino acid was the important determinant for efficient drug conversion. This was exemplified by the fact that residues with a molecular volume of greater than ~166 $Å^3$ were at least 3-fold less efficient at CPT-11 catalysis (Table 3). We hypothesize that the large substituents of these amino acids project into the active site and minimize the availability of the catalytic triad to the substrate or that the residues significantly impede passage of cleaved substrate through the side door. We are currently performing NMR structural studies with the purified proteins to assess which mechanism is responsible for inhibited drug metabolism.

With the L362 mutation, the hydrophobicity and charge of this amino acid appear to be the determinant factors for CPT-11 activation. As indicated in Table 2, inhibition of drug

catalysis was only observed following replacement with Lys or Arg. Interestingly, no effect on CPT-11 or *o*-NPA catalysis was observed following substitution of L362 with His. We analyzed the dipole moment of CPT-11 and determined that the piperidino rings were more positively charged than the rest of the molecule. Thus, we propose that the clash between the positive charges on residue 362 and CPT-11 would contribute to the significant decrease in the affinity and reaction velocity of L362R pnb CE toward this substrate.

We also created mutations at the corresponding side-door residues in rCE. Substitution of both the L252 and L424 residues (corresponding to S218 and L362, respectively) to Arg residues resulted in inhibited CPT-11 metabolism. These data are consistent with those observed with the pnb CE mutants. Thus, pnb CE was not only significantly structurally homologous to rCE, as represented by the 2.4 Å rmsd variation along the 400 residues of the α-carbon trace within the two proteins, but also significantly functionally homologous. This is further supported by the similar kinetic parameters of rCE (*28*) and pnb CE with *o*-NPA. Both enzymes exhibit Michaelis−Menten kinetics with *o*-NPA, with a K_m value of 586 μM and a V_{max} value of 88.3 μmol min^{-1} mg^{-1} for rCE and a K_m value of 701 μM and a V_{max} value of 84.6 μmol min^{-1} mg^{-1} for pnb CE. The rabbit CE has a slightly higher catalytic efficiency of 153 s^{-1} mM^{-1} than pnb CE (108.71 s^{-1} mM^{-1}). With CPT-11, there is a 6-fold difference in the catalytic efficiency between rCE (3 s^{-1} mM^{-1}) and pnb CE (0.5 s^{-1} mM^{-1}). On the basis of these observations, we can conclude that pnb CE is a valuable model for studying substrate catalysis by mammalian CEs, and allows rapid generation and evaluation of a large number of mutations for their ability to affect CPT-11 metabolism.

The analysis of the kinetic parameters for the wild-type and L362R pnb CEs demonstrated that the enzymes followed Michaelis−Menten kinetics when *o*-NPA was used as a substrate. However, both proteins exhibited allosteric kinetics with CPT-11. On the basis of analysis using the Monod−Wyman−Changeuw model (inset of Figure 3), both enzymes had three CPT-11 binding sites, and both exhibited positive binding cooperativity among these sites, which was not affected by the mutation. These findings are in good agreement with our observation that pnb CE exists primarily as a trimer in solution.

For a more detailed enzymatic analysis of both the wild-type and L362R mutant pnb CEs, we studied the viscosity dependence of the kinetic parameters using both substrates. Since low-molecular weight viscogens such as glycerol or sucrose can hinder the diffusion of small molecules, these reagents will decrease the rate of those reactions that are limited by substrate association or product release (*24*, *29*, *30*). Our studies revealed that the second-order rate constant for *o*-NPA catalysis was not sensitive to viscosity. This observation also confirmed that sucrose did not physically perturb pnb CE or the L362R mutant protein. However, the viscosity dependence of the k_{cat}/K_m value for CPT-11 hydrolysis clearly suggests that this process is limited by substrate association (Table 7).

On the basis of our kinetic analyses, we propose that the difference in enzyme kinetics with *o*-NPA and CPT-11 is due to the size difference between the two substrates. Since *o*-NPA is small in comparison to CPT-11, it can readily fit into the substrate-binding site, even if the enzyme is in the trimeric conformation. As a result, there is a direct correlation between the substrate concentration and reaction velocity until the enzyme is saturated, as reflected by the hyperbolic velocity curve. However, because of its larger size, the access of CPT-11 to the active site is hindered. This phenomenon is represented by the sigmoidal substrate−velocity curve that we observed with L362R pnb CE and CPT-11 (Figure 3). Allosteric behavior toward substrates has been observed with other CEs. For example, Suzuki-Kurasaki reported that the guinea pig liver microsomal deacylase is a hexameric protein, consisting of two trimers and six substrate-binding sites. This enzyme also exhibited allosteric enzyme kinetics with different substrates (*31*).

Overall, our studies indicate that pnb CE is a valuable model for studying CE-mediated CPT-11 metabolism by mammalian CEs. This model system provides a rapid screen for specific mutations that might affect drug metabolism. Furthermore, it will allow the facile production of ^{15}N- and ^{13}C-labeled wild-type and mutant proteins for structural studies by NMR. Since there is significant structural and functional homology between pnb CE and rCE, these studies should provide further insights into the mechanism of CPT-11 activation by mammalian CEs.

REFERENCES

1. Slichenmyer, W. J., Rowinsky, E. K., Donehower, R. C., and Kaufmann, S. H. (1993) The current status of camptothecin analogues as antitumor agents, *J. Natl. Cancer Inst. 85*, 271−291.
2. Houghton, P. J., and Santana, V. M. (2002) Clinical trials using irinotecan, *J. Pediatr. Hematol./Oncol. 24*, 84−85.
3. Friedman, H. S., Keir, S. T., and Houghton, P. J. (2003) The emerging role of Irinotecan (CPT-11) in the treatment of malignant glioma in brain tumors, *Suppl. Cancer 97*, 2359−2362.
4. Tanizawa, A., Fujimori, A., Fujimori, Y., and Pommier, Y. (1994) Comparison of topoisomerase I inhibition, DNA damage, and cytotoxicity of camptothecin derivatives presently in clinical trials, *J. Natl. Cancer Inst. 86*, 836−842.
5. Tsuji, T., Kaneda, N., Kado, K., Yokokura, T., Yoshimoto, T., and Tsuru, D. (1991) CPT-11 converting enzyme from rat serum: purification and some properties, *J. Pharmacobiol. 14*, 341−349.
6. Satoh, T., Hosokawa, M., Atsumi, R., Suzuki, W., Hakusui, H., and Nagai, E. (1994) Metabolic activation of CPT-11, 7-ethyl-10-[4-(1-piperidino)-1-piperidino]carbonyloxycamptothecin, a novel antitumor agent, by carboxylesterase, *Biol. Pharm. Bull. 17*, 662−664.
7. Potter, P. M., Pawlik, C. A., Morton, C. L., Naeve, C. W., and Danks, M. K. (1998) Isolation and partial characterization of a cDNA encoding a rabbit liver carboxylesterase that activates the prodrug Irinotecan (CPT-11), *Cancer Res. 52*, 2646−2651.
8. Satoh, T., and Hosokawa, M. (1998) The mammalian carboxylesterases: from molecules to functions, *Annu. Rev. Pharmacol. Toxicol. 38*, 257−288.
9. Oakshott, J. G., Claudianos, C., Russell, R. J., and Robin, G. C. (1999) Carboxyl/cholinesterases: a case study of the evolution of a successful multigene family, *BioEssays 21*, 1031−1042.
10. Hosokawa, M., Maki, T., and Satoh, T. (1990) Characterization of molecular species of liver microsomal carboxylesterases of several animal species and humans, *Arch. Biochem. Biophys. 277*, 219−227.
11. Brzezinski, M. R., Spink, B. J., Dean, R. A., Berkman, C. E., Cashman, J. R., and Borson, W. F. (1997) Human liver carboxylesterase hCE-1: binding specificity for cocaine, heroin, and their metabolites and analogs, *Drug Metab. Dispos. 25*, 1089−1096.
12. Bencharit, S., Morton, C. L., Xue, Y., Potter, P. M., and Redinbo, M. R. (2003) Structural basis of heroin and cocaine metabolism by a promiscuous human drug-processing enzyme, *Nat. Struct. Biol. 10*, 349−356.

13. Humerickhouse, R., Lohrbach, K., Li, L., Bosron, W., and Dolan, M. (2000) Characterization of CPT-11 hydrolysis by human liver carboxylesterase isoforms hCE-1 and hCE-2, *Cancer Res. 60*, 1189−1192.
14. Bencharit, S., Morton, C. L., Howard-Williams, E. L., Danks, M. K., Potter, P. M., and Redinbo, M. R. (2002) Structural insights into CPT-11 activation by mammalian carboxylesterases, *Nat. Struct. Biol. 9*, 337−342.
15. Danks, M. K., Morton, C. L., Krull, E. J., Cheshire, P. J., Richmond, L. B., Naeve, C. W., Pawlik, C. A., Houghton, P. J., and Potter, P. M. (1999) Comparison of activation of CPT-11 by rabbit and human carboxylesterases for use in enzyme/prodrug therapy, *Clin. Cancer Res. 5*, 917−924.
16. Khanna, R., Morton, C. L., Danks, M. K., and Potter, P. M. (2000) Proficient metabolism of CPT-11 by a human intestinal carboxylesterase, *Cancer Res. 60*, 4725−4728.
17. Xie, M., Yang, D., Wu, M., Xue, B., and Yan, B. (2003) Mouse liver and kidney carboxylesterase (M-LK) rapidly hydrolyzes antitumor prodrug Irinotecan and the N-terminal three-quarter sequence determines substrate specificity, *Drug Metab. Dispos. 31*, 21−27.
18. Beaufay, H., Amar-Costesec, A., Feytmans, E., Thines-Sempoux, D., Wibo, M., Robbi, M., and Berthet, J. (1974) Analytical study of microsomes and isolated subcellular membranes from rat liver. I. Biochemical methods, *J. Cell Biol. 61*, 188−200.
19. Wierdl, M., Morton, C. L., Weeks, J. K., Danks, M. K., Harris, L. C., and Potter, P. M. (2001) Sensitization of human tumor cells to CPT-11 via adenoviral-mediated delivery of a rabbit liver carboxylesterase, *Cancer Res. 61*, 5078−5082.
20. Albery, W. J., and Knowels, J. R. (1976) Evolution of enzyme function and the development of catalytic efficiency, *Biochemistry 15*, 5631−5640.
21. Fersht, A. (1983) *Enzyme Structure and Mechanism*, 2nd ed., W. H. Freeman, New York.
22. Horn, A., and Borning, H. (1969) Analysis of kinetic data of allosteric enzymes by a linear plot, *FEBS Lett. 3*, 325−329.
23. Nakatani, H. B. D. (1979) Meaning of diffusion-controlled association rate constants in enzymology, *J. Phys. Chem. 83*, 2662−2665.
24. Brouwer, A. C., and Kirsch, J. F. (1982) Investigation of diffusion-limited rates of chymotrypsin reactions by viscosity variation, *Biochemistry 21*, 1302−1307.
25. Zock, J., Cantwell, C., Swartling, J., Hodges, R., Pohl, T., Sutton, K., Rosteck, P., Jr., McGilvary, D., and Queener, S. (1994) The *Bacillus subtilis* pnb A gene encoding *p*-nitrobenzyl esterase: cloning, sequence and high-level expression in *Escherichia coli*, *Gene 151*, 37−43.
26. Gilson, M. K., Straatsma, T. P., McCammon, J. A., Ripoll, D. R., Faerman, C. H., Axelsen, P. H., Silman, I., and Sussman, J. L. (1994) Open "back door" in a molecular dynamics simulation of acetylcholinesterase, *Science 263*, 1276−1278.
27. Bartolucci, C., Perola, E., Cellai, L., Brufani, M., and Lamba, D. (1999) "Back Door" opening implied by the crystal structure of a carbamoylated acetylcholinesterase, *Biochemistry 38*, 5714−5719.
28. Wadkins, R. M., Morton, C. L., Weeks, J. K., Oliver, L., Wierdl, M., Danks, M. K., and Potter, P. M. (2001) Structural constraints affect the metabolism of 7-ethyl-10-[4-(1-piperidino)-1-piperidino]-carbonyloxycamptothecin (CPT-11) by carboxylesterases, *Mol. Pharmacol. 60*, 355−362.
29. Blacklow, S. C., Raines, R. T., Lim, W. A., Zamore, P. D., and Knowles, J. R. (1988) Triosephosphate isomerase catalysis is diffusion controlled. Appendix: Analysis of triose phosphate equilibria in aqueous solution by ^{31}P NMR, *Biochemistry 27*, 1158−1167.
30. Mattei, P., Kast, P., and Hilvert, D. (1999) *Bacillus subtilis* chorismate mutase is partially diffusion-controlled, *Eur. J. Biochem. 261*, 25−32.
31. Suzuki-Kurasaki, M., Yoshioka, T., and Uematsu, T. (1997) Purification and characterization of guinea-pig liver microsomal deacetylase involved in the deacylation of the O-glucoside of N-hydroxyacetanilide, *J. Biochem. 325*, 155−161.

BI035586R